Experiments of Plasma Current Start-Up in Tokamak-Helical Hybrid Device TOKASTAR-2*)

Makoto HASEGAWA, Kozo YAMAZAKI, Hideki ARIMOTO, Tetsutarou OISHI, Kazuhisa BABA, Motoki SUWABE and Tatsuo SHOJI

Department of Energy Engineering and Science, Graduate School of Engineering, Nagoya University, Furo-cho, Chikusa-ku, Nagoya 464-8093, Japan

(Received 7 December 2010 / Accepted 17 August 2011)

The small device named TOKASTAR-2 has tokamak-helical hybrid coils to generate both configurations independently. We produced pre-ionized plasma with simple toroidal field in this TOKASTAR-2, and the spatial profiles of electron temperature and density were measured, which suggests both fundamental ECR heating process and other heating mechanisms. Within the limitation of static vertical field, around 0.1 kA plasma current was induced with strongly inward shifted configuration observed by the fast camera measurement, which is verified by the TOSCA equilibrium analysis. It was found that the eddy currents on the vacuum chamber prevent the plasma current build-up. The preliminary application of outer helical field was tried and the plasma current reduction was observed. For the optimization of tokamak operation to drive 1 kA plasma current, time-varying vertical field coil currents and eddy currents were evaluated by the TOSCA code, and the necessity of in-vessel vertical field coils was clarified. The pure current-less TOKASTAR configuration will be demonstrated by installing additional helical coils in the future.

Keywords: TOKASTAR-2, Tokamak, Helical, hybrid configuration, plasma current, pre-ionized plasma, Langmuir probe, ECR (Electron Cyclotron Resonance), UHR (Upper Hybrid Resonance), TOSCA code

DOI: 10.1585/pfr.6.2402141

1. Introduction

Some combinations among tokamak and helical configurations have been proposed for a compact steady-state system without plasma current disruptions. Moreover, coil arrangement with reduced helical coil numbers in the hybrid design has been proposed for enough plasma-coil space and easy reactor maintenance. TOKASTAR configuration [1] is one of compact tokamak-helical hybrid confinement systems. We proposed an N(toroidal mode number) = 1 or $N = 2$ compact coil system C-TOKASTAR (Compact Tokamak/Stellarator Hybrid) without toroidal coil system [2, 3]. This system has several advantages: (1) steady-state operation by helical coils, (2) no current disruption risk by external helical field application, (3) probable high-beta achievement by strong magnetic well, (4) enough divertor space by simple coil configuration, (5) compact economic system by spherical configuration, and (6) easy maintenance by simple $N = 1$ or $N = 2$ coil system. Based on the achievement of C-TOKASTAR, a new small device named "TOKASTAR-2" was designed and constructed [3, 4]. Different from the C-TOKASTAR coil system, the toroidal field coil system is added in the TOKASTAR-2 (Fig. 1) to generate both tokamak and helical configurations independently.

One of main purposes of the present TOKASTAR-2 experiment is to investigate the effects of outer helical field application on tokamak plasmas. The coil configuration of this device is shown in Fig. 1. TOKASTAR-2 consists of four kinds of coils and one type of supplemental coils; eight 50-turn toroidal field (TF) coils, three ohmic heating (OH) coils, a pair of 100-turn vertical field (VF) coils and a pair of 98-turn outer helical field (HF) coils. The additional helical coils (AHF) with sector shape located upside and down-side [4] are required to reproduce original pure current-less TOKASTAR configurations. TF, OH and HF coil systems are installed inside the vacuum chamber, and AHF coil system is not installed yet. Radio Frequency (RF) wave having the frequency of 2.45 GHz is used to

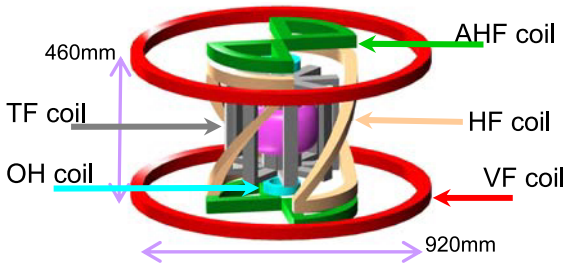

Fig. 1 Coil configuration of TOKASTAR-2. AHF (Additional Helical Coil) is not installed.

author's e-mail: hasegawa-makoto10@ees.nagoya-u.ac.jp

*) This article is based on the presentation at the 20th International Toki Conference (ITC20).

produce plasmas by the fundamental Electron Cyclotron Resonance (ECR) heating taking place at 875 G. The first plasma was produced in June 2009.

The TOKASTAR-2 experiment is characterized by four stages; (i) the production of pre-ionized plasma with simple torus field and the measurement of basic plasma parameters, (ii) the plasma current induction by using OH and VF coil systems and the optimization of tokamak operation, (iii) the HF application to investigate the effect on tokamak plasma, and (iv) the current-less Tokastar configuration generation by installing AHF coils. In this paper we focus on the experiments of stages (i) and (ii), and add preliminary data of stage (iii).

2. Spatial Profile of Pre-Ionized Plasmas

Pre-ionized plasmas were produced by RF injection (O-mode) into simple toroidal field configuration using pulse TF coil system. The maximum TF coil current (I_{TF}) was set 90 A so that toroidal field of 875 G is generated

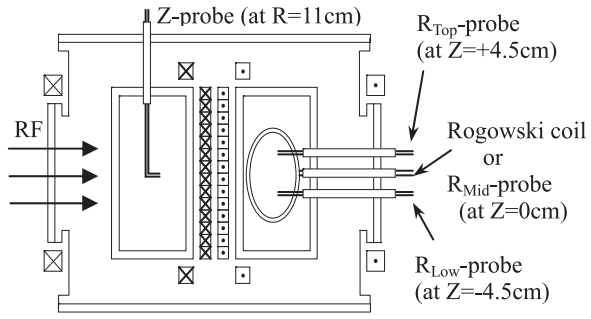

Fig. 2 Schematic layout of measurement instruments.

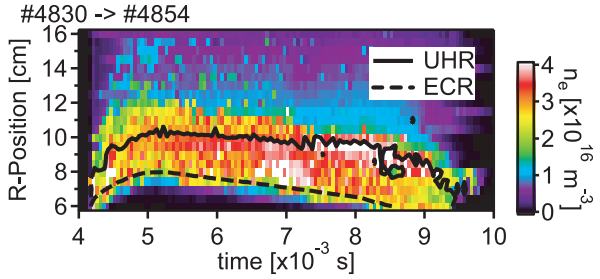

Fig. 3 Radial profile of electron density at mid plane.

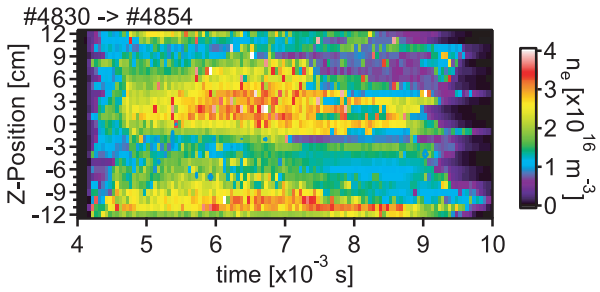

Fig. 4 Vertical profile of electron density at $R = 11$ cm.

at major radius R~8 cm. RF wave having the power of 0.6 kW was injected continuously. Spatial profiles of electron temperature (T_e) and electron density (n_e) were measured by using triple probes (direct display system) [5]. Working gas was helium having the pressure P_{He}~3.75×10^{-3} Torr. Figure 2 shows the schematic layout of measurement instruments. Using R_{Mid}-probe in the major radius(R) direction, density and temperature profiles in the range of $R = 6$~16 cm at $Z = 0$ cm were measured. Using Z-probe in the vertical (Z) direction, profiles in the range of Z = -12~+12 cm at $R = 11$ cm were measured.

Figure 3 shows R-profiles of n_e. The broken line shows position of ECR layer evaluated by using field calculation code and the solid line shows position of Upper Hybrid Resonance (UHR) layer. The plasma was initiated near the fundamental ECR layer. However, the position of density peak was different from the position of ECR layer during the discharge. On the other hand, the UHR layer corresponded with the peak. Therefore it was considered the plasma production and sustainment are due to not only ECR but also other heating mechanisms. Electron Bernstein wave (EBW) excited by mode conversion at UHR layer might be considered as another plasma heating process. The mode conversion rate and the absorption coefficient of EBW are now under calculation.

Figure 4 shows Z-profile of n_e. It is found that main plasma profile shifted vertically upward. It is considered due to the influence of error field. There were additional two dense regions above ($Z > 12$ cm) and below (Z~-10 cm) the main plasma. It is supposed that plasmas in these regions were produced by the ECR layers close to upper and bottom walls of TF coil.

3. Experimental Results of OH Plasmas

Plasma current start-up experiment in the ECR pre-ionized plasma described in the previous section, has been performed using OH and VF coil systems in the order of 10^{-5}~10^{-4} Torr pressure with helium gas. We could not obtain more than 0.1 kA plasma current within the limitation of static vertical field and with eddy currents strongly induced on the vacuum chamber.

Figure 5 shows typical waveforms of OH plasma operation; one-turn voltage at $R = 6$ and 18 cm, optical emission intensity measured by Avalanche Photodiode (APD) device, plasma current I_P measured by Rogowski coil at mid plane (shown in Fig. 2), electron temperature T_e and electron density n_e (measured at $R = 12$ cm and $Z = 0$ cm). Experimental condition was as follows; helium gas pressure $P_{He} = 9.1 \times 10^{-5}$ Torr, base pressure $P_{Base} = 6.8 \times 10^{-5}$, I_{TF}~90 A, static vertical coil current $I_{VF} = 7.5$ A (B_v~15 G), and RF power 0.8 kW (O-mode). The optical emission intensity and the plasma current I_P increased just after the onset of one-turn voltage, and I_P reached up to 98 A. At the same time, both T_e and n_e increased up to 70 eV and 2.5×10^{17} m^{-3}, respectively. The electron den-

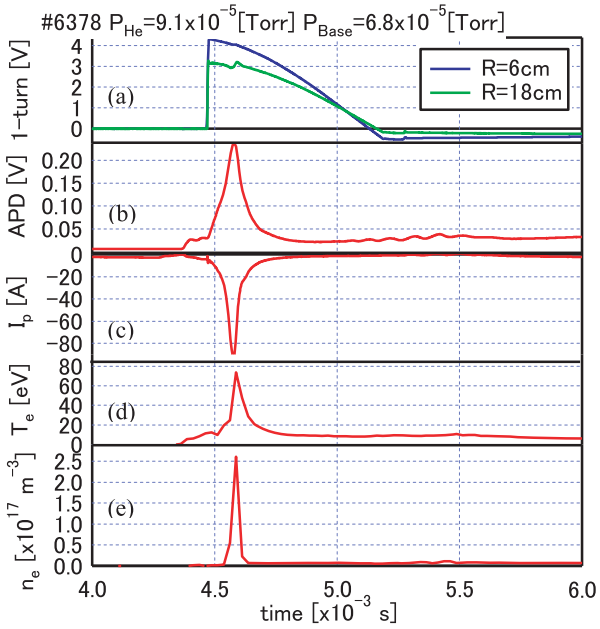

Fig. 5 Waveform of typical OH plasma operation. (a) one-turn voltage, (b) optical emission intensity, (c) plasma current I_p, (d) electron temperature T_e, and (e) electron density n_e.

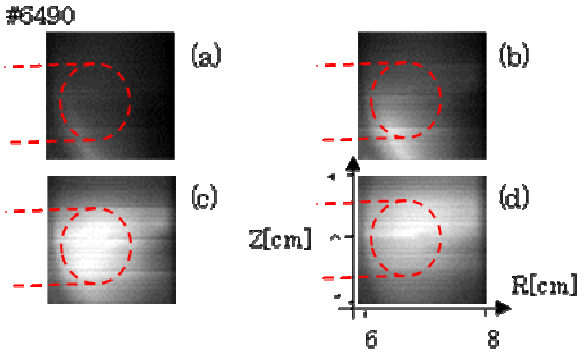

Fig. 6 Consecutive photographs of plasma by fast camera. Time interval is 24.7 μs, and the photo (c) corresponds to the plasma current maximum. The broken lines denote TOSCA results almost same as shown in Fig. 13 (b).

sity exceeded the cut-off density (0.7×10^{17} m^{-3}) of pre-ionized 2.45 GHz ECH plasma produced in TOKASTAR-2.

Photographs of OH plasma are shown in Fig. 6. Figure 6 (a), (b), (c) and (d) are continuous photographs taken by fast camera (40500 fps) with time interval of 24.7 μs. Experimental conditions were $P_{He} = 3.0 \times 10^{-4}$ Torr, $P_{Base} = 6.5 \times 10^{-5}$ Torr, $I_{VF} = 7.5$ A (static), and the injected RF power of 0.7 kW. In this shot, plasma current (I_P) reached up to 54 A. It is turned out from Fig. 6 (a)~(d) that the OH plasma moved vertically upward. This movement is supposed to be due to up-down unbalance of induced eddy current and applied static vertical field and is the cause of plasma current decay. It may be

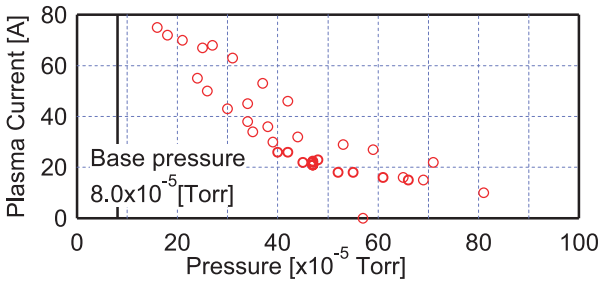

Fig. 7 Plasma current vs. helium gas pressure.

caused by error field and the plasma may be cooled down by impurity radiation. At present, the static vertical field in this shell-less tokamak is inappropriate to suppress the horizontal displacement due to time-varying hoop force, which can also cause plasma current decay. The analysis on the equilibrium using time-varying vertical field will be discussed in Section 5.

We measured plasma currents with varying the gas pressure. Figure 7 shows pressure dependence of induced plasma current. At this time, base pressure was $P_{Base} = 8.0 \times 10^{-5}$ Torr and other parameters were the same as those in Fig. 6. The larger plasma currents were driven with lower helium pressure. However, it was difficult to produce plasmas in further lower pressure ($P_{He} < 1.6 \times 10^{-4}$ Torr). The gas recycling may contribute to the density increase during the plasma current build-up. It is considered that induction of larger I_p need improving vacuum and wall conditions.

4. Helical Field Effects on Plasma Current Reduction

Lastly, we tried applying static outer helical field on OH plasmas. Experimental condition was the same as the experiment of Fig. 5 except higher gas pressure $P_{He} = 4.0 \times 10^{-4}$ Torr. Figure 8 shows plasma currents with varying static HF coil current (I_{HF}). Plasma currents (I_p) decreased as I_{HF} increased. In comparison with I_p at $I_{HF} = 0$ A, I_p decreased to 82.4 % at $I_{HF} = 5$ A and 30.3 % at $I_{HF} = 10$ A. We suspected vertical field made by outer HF coils contributed to the decrease of I_p. The ratios of B_v (VF+HF) to B_v (VF) in toroidal direction are shown in Fig. 9, where B_v (VF+HF) and B_v (VF) indicate vertical fields made by VF coils and HF coils and by only VF coils respectively. The variation of B_v (VF+HF) at $I_{HF} = 5$ A is between ±11.5 % and that at $I_{HF} = 10$ A is ±23 %. Therefore we evaluated reduction of I_p when vertical field varies. Figure 10 shows I_p varying static I_{VF} without helical field. According to Fig. 10 with line fitting, ±11.5 % of I_{VF} fluctuation gives $0.91 I_p$ and ±23 % of I_{VF} variation gives $0.825 I_p$ compared with maximum I_p at $I_{VF} = 7.5$ A. These I_p reduction rates by varying I_{VF} do not correspond with those of application of I_{HF} in Fig. 8.

The magnetic line tracing analyses revealed the influence of helical field on magnetic surface destruction. We

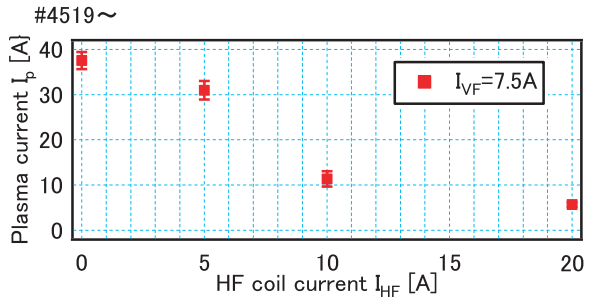

Fig. 8 Plasma current reduction by applying outer helical field.

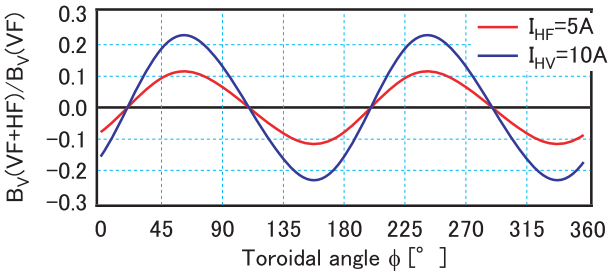

Fig. 9 $B_v(= Bz_{HF} + B_{VF})/B_v(\mathrm{VF})$ in toroidal direction.

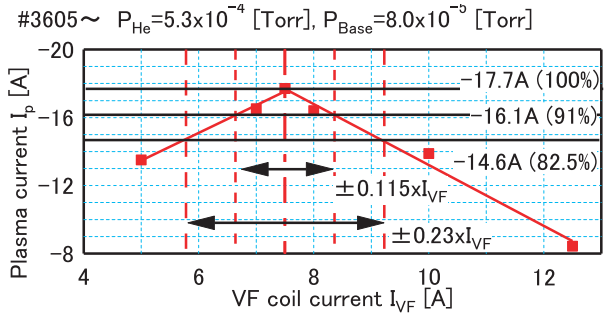

Fig. 10 I_p with varying I_{VF}. Arrows indicate the range of variation of B_v(VF + HF) in Fig. 9.

made Poincare plots of magnetic lines near the plasma boundary and obtained the decrease in area of the last closed surface which may be related to the decrease in I_p. The detailed analyses are now under investigation.

5. Equilibrium Analysis using TOSCA Code

Presently we use a DC power supply for VF coils, however, we intend to use pulsed current by capacitors. Using TOSCA code, we evaluated required VF coil current and induced eddy current on the vacuum chamber. The TOSCA (Tokamak Operation Scenario and Circuit Analysis) code [6] is free-boundary equilibrium analysis code which is suitable to design tokamak experiment device. It can calculate the best vertical coil current to achieve target plasma parameters for given location of poloidal coils. In equilibrium calculation, Grad-Shafranov equation with discrete mesh is solved.

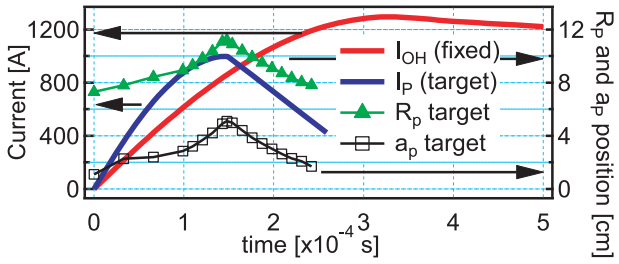

Fig. 11 Input waveforms of OH and plasma currents (I_{OH}, I_p), and major and minor plasma radii (R_p, a_p).

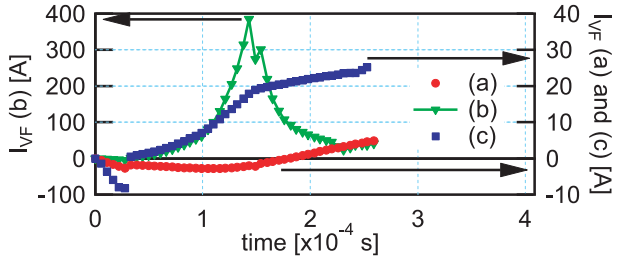

Fig. 12 Calculated I_{VF} of (a), (b) and (c).

OH and VF coils were divided into several coil blocks and the vacuum chamber was divided into 62 conductor blocks. We assumed $7.2\times10^{-7}\,\Omega\,\mathrm{m}$ (stainless) for the resistivity of the vacuum chamber. The waveform of OH coil current (I_{OH}) measured in experiments was used as input wave form. Figure 11 shows waveforms of input parameters as follow: OH current (I_{OH}), plasma current (I_P), plasma major radius (R_P) and plasma minor radius (a_P). Since we did not measure detailed profile of parameters experimentally, we assumed that the plasma current density j was parabolic, the internal inductance l_i was 1.0 and the poloidal beta β_p was almost zero.

Using above input parameters, three types of simulation were carried out,

(a) without vacuum chamber
(b) with vacuum chamber and VF coils located outside the chamber (present status of TOKASTAR-2).
(c) with vacuum chamber and VF coils installed inside chamber (future plan).

Figure 12 shows calculated VF current I_{VF} of cases (a), (b) and (c), and Fig. 13 shows magnetic flux surfaces of cases (a), (b) and (c) at $I_P = 1.0\,\mathrm{kA}$.

(a) To achieve target value of I_p, the VF coil current I_{VF} was within ±5 A. The plasma was located slightly outside the center of TF coil.

(b) Under the existence of the vacuum chamber, plasma major radius R_p becomes small. The pulsed VF coil current I_{VF} needed short duration and large temporal evolution up to 450 A at maximum. It was considered that eddy currents on the vacuum chamber give strong influences on plasma equilibrium.

(c) Plasma parameters had better agreement with tar-

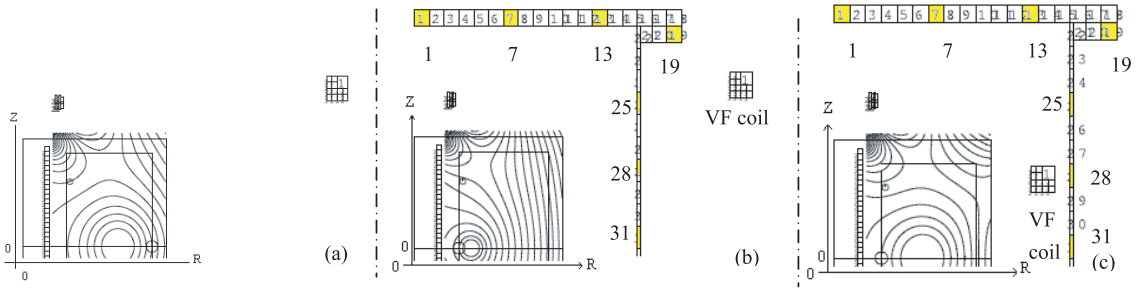

Fig. 13 Magnetic flux surfaces of (a) without vacuum chamber (VC), (b) with VC and outer VF coil, and (c) with VC and inner VF coil.

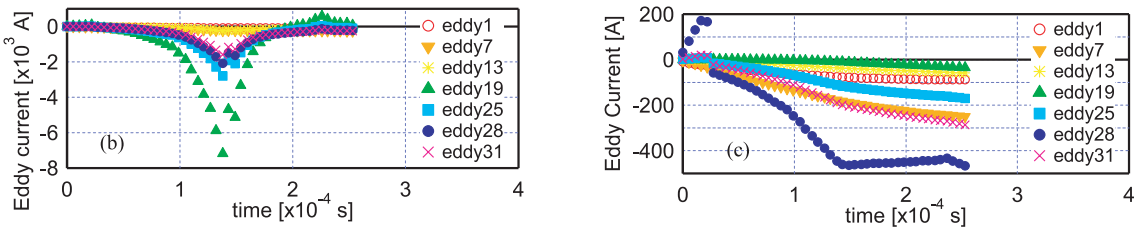

Fig. 14 Typical eddy currents of cases (b) and (c).

get values compared with (b) and the calculated I_{VF} was about 25 A. This value is within the present coil design limitation.

In the cases of (a) and (b), calculated R_p and a_p disagree with assumed target values in Fig. 11. TOSCA has higher priority for achieving target I_p value compared than achieving target R_p and a_p values. The hoop forces in cases (a), (b) and (c) were almost same because the same target I_p value was used. However vertical fields B_z applied to the plasma were different; (a) $B_z = 15$ G, (b) $B_z = 40$ G and (c) $B_z = 18$ G. Therefore, R_p shifts to balance the force of $I_p \times B_z$ with the hoop force.

Next, we compared eddy currents. Figure 14 shows eddy currents of cases (b) and (c). In this figure eddy1, eddy7, eddy13, ...eddy31 indicate conductor element numbers shown in Fig. 13. Eddy current of eddy19 in (b) achieves 7,000 A. However maximum eddy current of eddy28 in case (c) was suppressed down to 450 A. The waveforms of eddy19 in case (b) and eddy28 in case (c) are similar to each waveforms of calculated I_{VF} shown as traces (b) and (c) in Fig. 12. From this result, it was turned out that short-pulsed I_{VF} contributes to enlarge the eddy current.

In the case of in-vessel VF coils, the larger eddy current is expected as VF coils are installed nearer the vacuum chamber. Finally it reaches few thousand of amperes if VF coils are attached inner wall of chamber. Installing VF coils inside the vacuum chamber has an advantage reducing the required I_{VF}, and the improper location of VF coils leads to the extreme high eddy current and the increase in I_{VF}.

It was turned out that present VF coils outside vacuum vessel is inappropriate for the present shell-less tokamak operation. We plan to check different locations of VF coils inside the vacuum chamber and to adjust the waveform of target I_P so that the waveform of I_{VF} becomes gradually changing. We are also going to install conducting copper shell for equilibrium assistance.

6. Conclusions

We started plasma confinement experiments with TOKASTAR-2 device with outer helical coils, and came to the following conclusions:

(1) From the spatial profile of pre-ionized plasma, it was found that the plasma density peak in the R-direction did not correspond with the location of the ECR fundamental layer. Other mechanism such as electron Bernstein wave heating should be taken into account.

(2) In experiments using OH coils, we obtained 0.1 kA plasma current within the limitation of static vertical field. From photographs taken by fast camera, it was clarified that OH plasma moved vertically upward. The size and position of the plasma light agrees with the equilibrium analysis with eddy current on the vacuum chamber.

(3) Plasma current was reduced when the present helical field was applied to OH plasma. The edge magnetic surface was destroyed and plasma column shrinked, which was suggested in vacuum magnetic field line tracing calculation. The full helical field application is required by installing AHF coils.

(4) By the equilibrium analysis using TOSCA code, present VF coils outside the vacuum chamber needs time-varying I_{VF} with large amplitude and short duration. On the contrary, installing VF coils inside the vacuum chamber has possibility to optimize I_{VF} to have small value and gradual temporal evolution. We plan to check other locations of VF coils in the vacuum chamber and compose a new power supply based on the simulation results.

To make higher plasma current operation, we are planning to install in-vessel vertical field coils with pulsed power system and/or to install stabilizing conductive shell. To demonstrate pure current-less TOKASTAR confinement concept, we will add additional helical field (AHF) coils in the near future.

[1] K. Yamazaki and Y. Abe, *Tokastar: Tokamak-Stellarator Hybrid with Possible Bean-Shaped operation*, Research Report of the Institute of Plasma Physics, Nagoya, Japan, IPPJ-718 (1985).
[2] K. Yamazaki and Y. Kubota, Proceedings of Plasma Science Symposium 2005 and the 22nd Symposium on Plasma Processing (PSS2005/ SPP-22) (26-28 January 2005, Nagoya Japan) P3-094 (2005).
[3] K. Yamazaki, Y. Taira, T, Oishi, H. Arimoto and T. Shoji, J. Plasma Fusion Res. SERIES **8**, 1044 (2009).
[4] T. Oishi, K. Yamazaki, K. Okano, H. Arimoto, K. Baba, M. Hasegawa and T. Shoji, J. Plasma Fusion Res. SERIES **9**, 69 (2010).
[5] S.L. Chen and T. Sekiguchi, J. Appl. Phys. **36**, 2363 (1965).
[6] K. Shinya, Private communication.